

Introduction

Airborne electromagnetics (AEM) continues to be a popular choice for mineral exploration and increasingly in other industries such as oil and geothermal exploration; however, three-dimensional inversion of large-scale time domain surveys remains a difficult endeavour. When AEM data is collected over thin conductive targets, a conventional voxel-based inversion (e.g. Haber and Schwarzbach, 2014) can encounter difficulties. Not only is the problem computationally intense due to many source locations spread over a large area, but the end goal is for the inversion to produce sharp contrasts in conductivity over narrow regions. With L2 and even L1 type regularization, this task is not always feasible, and alternative methods to assist this process are sought.

One option is to incorporate parametric methods (e.g. Dorn et al., 2000), where a reduced set of parameters is defined that describes an anomalous resistivity distribution, and we invert for these optimal parameters. We can also combine level sets (Osher and Sethian, 1988) with parametric methods (Aghasi et al., 2011) to locate the size, shape and magnitude of an individual resistive or conductive anomaly (McMillan et al., 2014). We extend the parametric level set approach to include multiple conductors in order to produce a general method suitable for more complex geologic scenarios.

Parametric Inversion Theory

This research focuses on time-domain electromagnetics, and as such we start with Maxwell's equations in time using the quasi-static approximation

$$\nabla \times \mathbf{E} + \mu \frac{\partial \mathbf{H}}{\partial t} = 0 \quad (1)$$

$$\nabla \times \mathbf{H} - \frac{1}{\rho} \mathbf{E} = \mathbf{s} \quad (2)$$

where \mathbf{E} is electric field, \mathbf{H} is magnetic field, t is time, μ is magnetic permeability, ρ is electrical resistivity, and \mathbf{s} is a source term. We take Equations 1 and 2, and implement a finite-volume discretization on OcTree meshes (Haber and Heldmann, 2007) with the goal of finding best fitting anomalies in a smooth background. A smooth background can mean a uniform half-space or a heterogeneous resistivity distribution from a previous inversion result.

Each anomalous body is based on a 3D skewed ellipsoid controlled by nine free parameters. These degrees of freedom are the central location of the ellipsoid, the radius in each Cartesian direction, and three skewing parameters which can contort the anomaly in any direction. We then calculate a level set function τ_i in each mesh cell for every anomaly i , defined as

$$\tau_i = c - \hat{\mathbf{x}}_i^T \mathbf{M} \hat{\mathbf{x}}_i \quad (3)$$

where c is a positive constant, $\hat{\mathbf{x}}_i$ is the three-dimensional Cartesian central location of the anomaly, and \mathbf{M} is a 3 x 3 symmetric positive definite matrix with six independent skewing and radius parameters. Each level set τ_i is passed through an analytic step function, as shown in Equation 4, to compute the variable w_i in each mesh cell

$$w_i = 1 - \frac{1}{2}(1 + \tanh(a\tau_i)) \quad (4)$$

where the variable a controls the steepness of the step function. When $w = 0$, this corresponds to an anomalous resistivity region (ρ_1), and when $w = 1$, it represents a background resistivity region (ρ_0). In Equation 4, we have applied the hyperbolic tangent as the analytic step function, but other choices such as the inverse tangent could also be used (Tai and Chan, 2004). To calculate the resistivity in each mesh cell, we incorporate all level set functions through Equation 5, where n is the number of anomalous bodies in the inversion. Care must be taken when choosing the value of n as the inversion could underestimate or overestimate the true number of anomalies present. For the examples in this research, n is chosen to be three based on examination of the data.

$$\rho(\rho_0, \rho_1, w_i) = \rho_0 + \left(1 - \prod_{i=1}^n w_i\right)(\rho_1 - \rho_0) \quad (5)$$

We use a Gauss-Newton optimization schedule as outlined in Oldenburg et al., (2013), and the parameters are scaled to improve the conditioning of the system.

Synthetic Example

To demonstrate the multiple body parametric inversion, we constructed a synthetic example based on a time-domain coincident loop AEM field data set over a greenstone belt area, where multiple thin dipping conductors exist in a resistive background. The coincident loop system from the field data, VTEM, is discussed in more detail in various works (e.g. Allard, 2007). For consistency, we will state all resistivity values in units of Ohm-meters (Ωm). In the synthetic model, each anomaly is assigned a resistivity of $0.2 \Omega\text{m}$ in a background of $1000 \Omega\text{m}$. The two northern conductors have a dip of 60 degrees to the North-West, and the South-East anomaly has a vertical dip of 90 degrees. The survey lines are collected with a heading of 310 degrees, and there are 508 transmitter locations with dBz/dt measurements from 20 time channels between $150 \mu\text{s}$ and $3180 \mu\text{s}$. The nominal line spacing is 120m, with a few lines separated by 60m in the North-East region. Prior to inversion, 5% Gaussian noise is added to the data. Our starting guess presumes no apriori information and consists of three 200m radius spheres located in the center of each of the anomalous zones at an elevation of 150m (depth of 200m). A plan map of the first time channel along with data locations in black and the outline of the starting guesses in white is shown in Figure 1a. The true model in plan view is displayed in Figure 1b and in cross-section at a constant y value of 7332810 in Figure 1c. We presume to know the true resistivities of the three anomalies and the background in this trial.

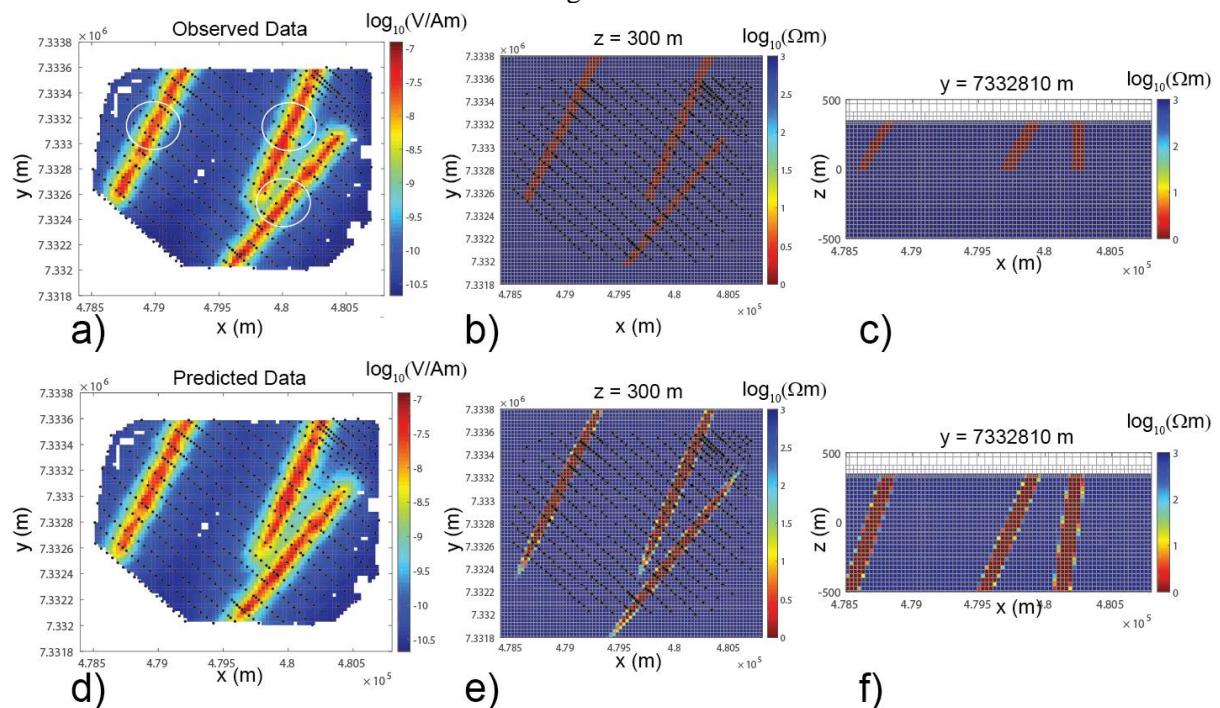


Figure 1 Multiple body parametric inversion over a synthetic example containing three linear conductors with data locations shown as black dots. a) Observed dBz/dt data at $150 \mu\text{s}$ with starting guesses for the anomalies outlined as white circles b) Plan view of true model at an elevation of 300m (50 m depth) c) Cross-section through the true model at a constant y value of 7332810 d) Predicted dBz/dt data at $150 \mu\text{s}$ e) Plan view of parametric inversion at an elevation of 300m f) Cross-section through the parametric inversion at a constant y value of 7332810

The inversion takes 37 Gauss-Newton iterations before it is unable to find a step that reduces the data misfit by more than 0.1%, and this is taken as our final model. The predicted data at the first time channel is portrayed in Figure 1d, and a plan view and cross-section through the recovered parametric model are shown in Figure 1e and 1f respectively. The predicted data compares well with the observed data, and the parametric inversion produces three linear conductors in the correct location in plan view. In cross-section the anomalies extend to greater depth compared to the true model, but the interpreted dip of each anomaly is approximately correct, although the vertical conductor is interpreted to have a slight dip to the North-West. In general, the results are encouraging and we continue with the field example.

Field Example

To test the multiple body parametric inversion on a field data set, we use the aforementioned greenstone field example. The survey layout and time channels are the same as the synthetic example and the observed data from the first time channel are shown in Figure 2a. The starting guess for the inversion is shown in plan view in Figure 2b and in cross section along a constant y value of 7332810 in Figure 2c. Once again the anomalies are assigned a resistivity of $0.2 \Omega\text{m}$ in a background of $1000 \Omega\text{m}$, but unlike the synthetic case, the optimal resistivity values are variables in the inversion. After 58 Gauss-Newton iterations, the predicted data from the first time channel is shown in Figure 2d, as well as a plan view and cross-section look through the parametric inversion in Figure 2e and Figure 2f respectively. The inversion returns optimal resistivities of $\rho_1 = 1.01 \Omega\text{m}$ and $\rho_0 = 1520 \Omega\text{m}$. To date, little is known regarding the true dip of the three conductors, but this research suggests they are all near-vertical in nature with the North-East anomaly having a slight dip to the South-East while the other two conductors dip gently to the North-West. As the predicted data does not have a perfect fit with the observed data, future work will look at using this result as an initial and reference model for a conventional voxel based inversion. This would allow additional features to enter the model space, while allowing the dip and resistivity within each anomaly to change if necessary.

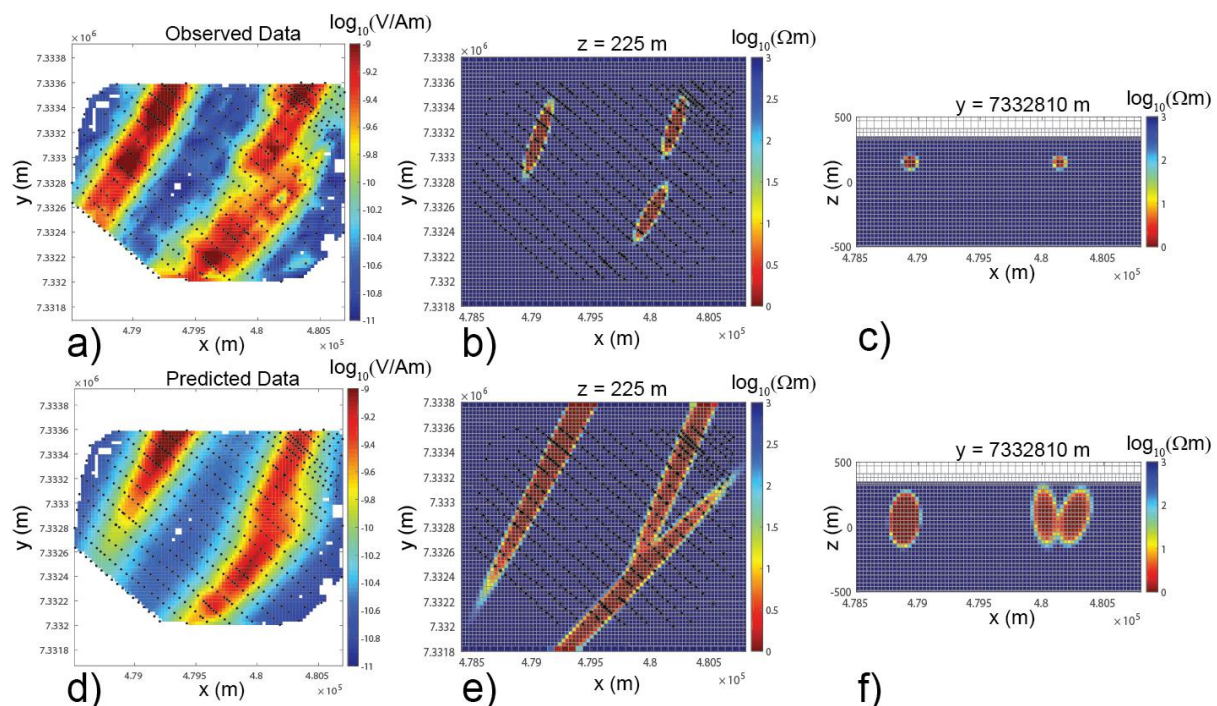


Figure 2 Multiple body parametric inversion over a field example with data locations shown as black dots. a) Observed dBz/dt data at $150 \mu\text{s}$ b) Plan view of starting model at an elevation of 225m c) Cross-section through the starting model at a constant y value of 7332810 d) Predicted dBz/dt data at $150 \mu\text{s}$ e) Plan view of parametric inversion at an elevation of 225m f) Cross-section through the parametric inversion at a constant y value of 7332810

Conclusions

We developed a multiple body parametric inversion for time-domain AEM data, and we showcased its abilities through a synthetic and field data inversion to image three linear narrow conductors. The parametric anomalies in the inversion are skewed ellipsoids that can change location, radius and rotation in each of the three Cartesian planes. The synthetic example, constructed to emulate a greenstone field setting, successfully recovers the spatial location and approximate dip of each conductor, although the depth extent of the inversion anomalies is deeper compared to the true model. In the field example we image three near-vertical conductors and provide a new conductivity interpretation for the area. Currently little is known regarding the true size and dip of the anomalies, so it is difficult to evaluate the accuracy of the field inversion. Building upon these results, future tests will be done iterating the parametric results with conventional voxel based inversion codes in order to fit additional features in the data set. The parametric code will also be modified to allow each parametric anomaly to have its own unique resistivity value.

Acknowledgements

The authors thank members of UBC-GIF for their ongoing support and to the Natural Sciences and Engineering Research Council of Canada for their financial help.

References

- Aghasi, A., Kilmer, M. and Miller, E.L. [2011] Parametric level set methods for inverse problems. *SIAM Journal on Imaging Sciences*, **4**, 618-650.
- Allard, M. [2007] On the origin of HTEM species. *Proceedings of Exploration '07*, 355-373.
- Dorn, O., Miller, E.L. and Rappaport, C.M. [2000] A shape reconstruction method for electromagnetic tomography using adjoint fields and level sets. *Inverse Problems*, **16**, 1119-1156.
- Haber, E. and Schwarzbach, C. [2014] Parallel inversion of large-scale airborne time-domain electromagnetic data with multiple OcTree meshes. *Inverse Problems*, **30**, 1-28.
- Haber, E., Heldmann, S. and Ascher, U. [2007] Adaptive finite volume method for distributed non-smooth parameter identification. *Inverse Problems*, **23**, 1659-1676.
- McMillan, M.S., Schwarzbach, C., Oldenburg, D.W., Haber, E., Holtham, E. and Prikhodko A. [2014] Recovering a thin dipping conductor with 3D electromagnetic inversion over the Caber deposit. *84th Annual International Meeting, SEG, Expanded Abstracts*, 1720-1724.
- Oldenburg, D.W., Haber, E. and Shekhtman, R. [2013] Three dimensional inversion of multisource time domain electromagnetic data. *Geophysics*, E47-E57.
- Osher, S. and Sethian, J. [1988] Fronts propagating with curvature dependent speed: algorithms based on Hamilton-Jacobi formulations. *Journal of Computational Physics*, **79**, 12-49.
- Tai, X. and Chan, T. [2004] A survey on multiple level set methods with applications for identifying piecewise constant functions. *International Journal of Numerical Analysis and Modeling*, **1**, 25-47.